Percolation in alloys with thermally activated diffusion

H. Ouyang and B. Fultz
Division of Engineering and Applied Science 138-78, California Institute of Technology, Pasadena, California 91125

(Received 17 April 1989; accepted for publication 27 July 1989)

For diffusion in a real alloy, some concepts of formal percolation theory may need to be reconsidered because the "immobile" atoms are not truly immobile. Our Monte Carlo simulations of vacancy diffusion on *bcc* lattices show the existence of a relationship between the activation barrier heights for the vacancy-atom exchanges and the effective percolation threshold concentration. In the language of formal percolation theory, we have modeled this problem by varying the immobile species' barrier height from infinity to some finite value and calculating the resulting percolation threshold. When both species of atoms have a finite mobility, however, our results can be interpreted in terms of probabilities for vacancies to escape local clusters in a fixed amount of time. We find that the dynamical behavior undergoes a marked change above and below the formal percolation threshold, but the strength of the percolating cluster is much less important than in formal percolation theory.

I. INTRODUCTION

Percolation theory has been used to study many problems[1–5]; an entertaining account of some of these applications is provided in Ref. 3. Much previous work has been concerned with cluster sizes in an array of immobile atoms and finding the concentration threshold for the presence of a percolating cluster of infinite length. This article reports results of a study of the dynamics of vacancy percolation in a two-component *bcc* alloy. Our problem is equivalent to the classical percolation problem when one atomic species is immobile, because then the vacancy is able to explore only one cluster of the mobile species. An immobile species of atoms was used in a previous investigation of diffusion.[6] Here we have not assumed that one species of atoms was absolutely immobile, but is instead slower than the other species. Percolation was determined by whether the vacancy traveled over some specified distance in a fixed amount of time. A previous analytical treatment of solute atom correlation factors for alloys with different finite atom-vacancy exchange frequencies used the random walk theory[7–9] to show that as one species became immobile, the correlation factor for the other species went to zero approximately at the site percolation threshold. A different approach can give the correct qualitative behavior by employing the path probability method with the conversion from the ensemble average to the time average.[10]

It was our intention to study the phenomenon of vacancy percolation by employing a mechanistic model of the vacancy jump. We employed the activated state rate theory to determine vacancy-atom exchange rates.[11,12] Rate theories require an attempt frequency and an activation energy for exchange. We used the rate theory to provide a probability for each possible exchange of the vacancy with one of its nearest neighbors. In the Monte Carlo algorithms employed here, a random number was used to select an exchange from this set; for some algorithms this also included a random waiting time associated with each exchange. The Monte Carlo simulations continued for many steps, during which statistical data about the diffusion distance and time were obtained. It was our goal to determine which concepts of formal percolation theory remain useful in the case of thermally activated diffusion, and then interpret these concepts in terms of the vacancy-atom exchange mechanism.

II. MONTE CARLO SIMULATIONS

Our Monte Carlo simulations employed a three-dimensional *bcc* lattice with periodic boundaries. The crystal lattice was cubic in shape, and for an edge length of 100 it contained 250 000 atoms. The binary alloys had an initially random occupancy of their two components, A and B. A single vacant site was introduced at various sites in the alloy. In our simulations, each Monte Carlo step resulted in the exchange of the vacancy with one of its eight first nearest neighbors. A Boltzmann probability, P_i, was assigned to each candidate vacancy-atom exchange on the basis of the height of its saddle point energy, $E_{\rm sp}$,

$$P_i = \exp(-E_{\rm sp}),$$

where $E_{\rm sp}$ is in units of kT, and takes on two values: $E^A_{\rm sp}$ and $E^B_{\rm sp}$ for A and B atoms, respectively. Because the exchange probabilities depended only on the difference $E^A_{\rm sp} - E^B_{\rm sp}$, the activation energy $E^B_{\rm sp}$ was set equal to zero without loss of generality. (This merely causes the various P_i to differ by a common factor.) For simplicity, all interatomic interactions were taken to be zero; this ensured that the alloy remained random during the vacancy diffusion. Even our simplest Monte Carlo approach (algorithm I) can satisfactorily determine the sequence of exchanges, but there are different ways to obtain the time required for each vacancy-atom exchange. To test the importance of the waiting time distribution for each exchange,[13] we employed three different Monte Carlo algorithms.

Algorithm I: The exchange probability for each atom neighboring the vacancy was set equal to the Boltzmann factor, P_i, and using these P_i as weights, a random number was used to select one exchange. The time was obtained as a running sum of the inverse of the Boltzmann factors of the exchanges that occurred, without any consideration of a

 0021-8979/89/224752-04$02.40

waiting time distribution for the exchange. This algorithm was preferred because of its efficiency.

Algorithm II: The mean waiting time for each of the eight neighbors of the vacancy was included by choosing a random number, R_i (where $0 \leqslant R_i \leqslant 1$), for each atom-vacancy exchange. The time for the exchange, τ_i, was

$$\tau_i = -P_i^{-1} \ln R_i.$$

The exchange that occurred was the one with the minimum value of τ_i, and a running sum of these τ_i was used to obtain the time.

Algorithm III: The selection of the exchange was the same as algorithm I. The duration of the residence of the current site, τ_i, was

$$\tau_i = -\langle \tau_i \rangle \ln R_i,$$

and $\langle \tau_i \rangle$ was chosen by assuming that the vacancy exchanges with all nearest neighbors occur in parallel

$$\langle \tau_i \rangle^{-1} = \sum_j P_j,$$

where the summation is over all the eight atoms neighboring the vacancy. This approach is similar to the residence time method.[13–15]

We defined the concentration of fast B atoms at which the vacancy just diffused over the distance, l_c, in the time, t_c, as the effective percolation threshold, $p_c^{\text{eff}}(l_c, t_c, E_{\text{sp}}^A)$. With guidance from data such as those of Fig. 1, we chose a time, t_c, and a distance, l_c, for determining p_c^{eff}. In Fig. 2, for example, we set $t_c = 5.2 \times 10^5$. Although this choice was somewhat arbitrary, we explored different values of t_c, as described below. To determine the effect of E_{sp}^A on $p_c^{\text{eff}}(l_c, t_c, E_{\text{sp}}^A)$, we took the following approach. For each alloy of fixed concentration, a large saddle point energy was chosen for the first Monte Carlo run. By lowering this energy by 0.1 for each run, we found the saddle point energy for which the vacancy diffused over the distance l_c in the time t_c.

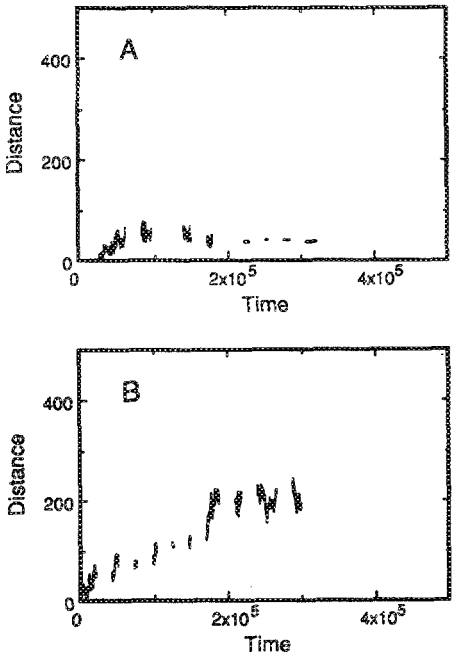

FIG. 1. Vacancy diffusion distance vs time for different concentrations: (A) $p = 0.28$ and (B) $p = 0.29$, with $E_{\text{sp}}^A = 10.0$, $E_{\text{sp}}^B = 0.0$.

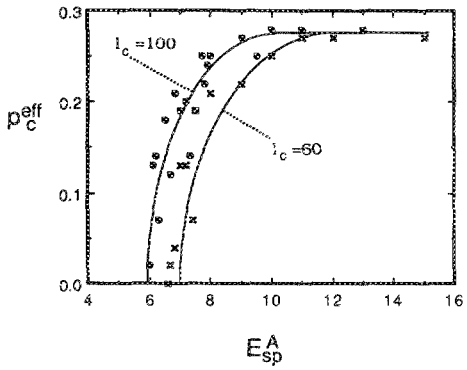

FIG. 2. Effective percolation threshold, p_c^{eff}, vs E_{sp}^A for different l_c and $t_c = 5.2 \times 10^5$. Lines are drawn to guide the eye.

III. RESULTS

At low concentrations of the fast B atom, watching on a video display terminal the vacancy motion in two-dimensional simulations on a square lattice showed that the vacancy became trapped within small clusters of B atoms. When the vacancy escaped from this cluster, it diffused irregularly until it became trapped again. This is the same sort of behavior that occurred in the three-dimensional simulations with the *bcc* lattice, as indicated in Figs. 1(a) and 1(b). The data of Figs. 1(a) and 1(b) were obtained with algorithm I, and the horizontal gaps in this plot occur when a slow A atom exchanges sites with the vacancy. The continuous segments in Fig. 1(a) occur when the vacancy moves within clusters of fast B atoms; the vertical dimensions of these continuous segments give a measure of the size of the cluster. As the concentration of B atoms increased from 0.28 and 0.29 in Fig. 1(b), the average cluster size and distance of diffusion increased. Similar results were obtained by using algorithms II and III. The use of the waiting time distributions led to more continuous curves than in Fig. 1, and the time scales were compressed by a factor of 3 or so. No qualitative changes in the percolation thresholds were found, however, and for convenience most of the results we present were obtained with algorithm I.

For the vacancy to travel a greater distance, the average cluster size of fast B atoms must be large, so a higher concentration of B atoms is required. This is expected from the percolation theory. Alternatively in the present problem, in order for the vacancy to travel a greater distance at a given concentration, E_{sp}^A must be reduced to make the slower A atoms more mobile. The part of the curve in Fig. 2 for low concentrations therefore shifts to the left with larger l_c.

On the other hand, when the distance, l_c, is specified, the time, t_c, required for the vacancy to travel this distance is shorter for smaller values of E_{sp}^A. For a given p_c^{eff} between 0 and 0.24, Fig. 3 shows that E_{sp}^A increases by a factor of about 2.3 each time t_c increases by a factor of 10 from 5.2×10^4 to 5.2×10^5 to 5.2×10^6. At higher concentrations ($p > 0.24$),

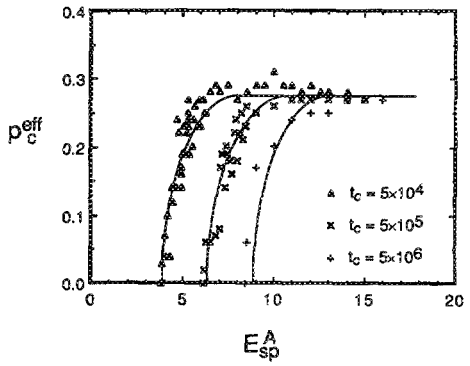

FIG. 3. Effective percolation threshold, p_c^{eff}, vs E_{sp}^A for $l_c = 80$ and different $t_c = 5.2\times10^4$, 5.2×10^5, and 5.2×10^6. Lines are drawn to guide the eye.

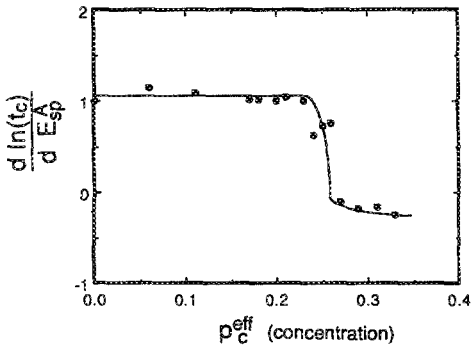

FIG. 5. Slope of lines in Fig. 4 vs p_c^{eff}. Line is drawn to guide the eye.

however, the vacancy can travel the distance, l_c, without being confined by slower A atoms because the cluster size of fast atoms is enlarged and an infinite percolating cluster appears. So at higher concentrations, the vacancy diffusion is less dependent on the activation energy, E_{sp}^A, of the slow A atoms, and the slopes of the curves in Fig. 3 approach zero.

For a fixed concentration, p_c^{eff}, and for a fixed distance criterion, l_c, the time, t_c, required to reach this distance depends on E_{sp}^A as shown in Fig. 4. The slopes of these curves,

$$d\left[\ln(t_c)\right]/dE_{\text{sp}}^A,$$

are presented in Fig. 5, where a discontinuity is evident near the concentration of 0.25. This concentration is close to the percolation threshold for the bcc lattice, $p_c = 0.243$, but we suggest that the discrepancy is due to the finite size of our lattice. In this way the critical behavior near the percolation threshold is still observed even when the diffusion of both species of atoms is thermally activated.

IV. DISCUSSION

Equating the Arrhenius expression for diffusivity, D, with the diffusivity from random walk theory gives

$$D = \langle l_c^2\rangle/\kappa t_c = D_0\exp(-\Delta E),$$

where D_0 and κ are constants, and ΔE is the controlling activation energy (in units of kT). In Fig. 4, l_c is kept constant, so

$$\ln(t_c) = \ln\left(\langle l_c^2\rangle/\kappa D_0\right) + \Delta E.$$

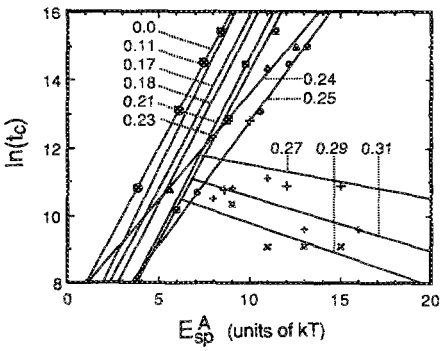

FIG. 4. Critical diffusion time, t_c vs E_{sp}^A for $l_c = 80$. Lines are least-square fit to the data.

Therefore

$$d\left[\ln(t_c)\right]/d(\Delta E) = 1.$$

In Fig. 5 we see that the slope,

$$d\left[\ln(t_c)\right]/dE_{\text{sp}}^A,$$

is nearly unity below $p = 0.24$. The rate-controlling activation energy in this low concentration regime, therefore, is E_{sp}^A. This is consistent with the vacancy mobility being controlled by the jump of an A atom bounding a cluster. We can estimate the time that the vacancy resides in a cluster of B atoms if we assume that escape from this cluster requires the exchange of the vacancy with one A atom. Given the opportunity for both V-A and V-B exchanges, the relative probability that the vacancy will exchange with an A atom is : $W \cong \exp(-E_{\text{sp}}^A)$. Using this relationship to predict the residence time in the cluster, we obtain a residence time of around 2×10^4 with $E_{\text{sp}}^A = 10$, in rough agreement with the data of Fig. 1. With algorithms II and III we obtained results essentially identical to those presented in Fig. 5.

For concentrations below p_c, we attempted to understand the vertical offset of the curves in Fig. 4 in terms of the change in mean cluster size near p_c. The time required for the vacancy to travel the distance l_c decreases as the cluster size increases. If we assume that the vacancy makes a random walk from cluster to cluster with a hopping frequency of $\exp(-E_{\text{sp}}^A)$, then we should expect a relationship between t_c and the mean cluster length, ℓ, of the form: $\ell^{-2} \propto t_c$. Although the mean cluster size is of fractal dimension, we have used the relationship[3]: $\ell^2 \propto |p - p_c|^{-1.8}$, valid for $p < p_c$, to obtain qualitatively the vertical shifts of Fig. 4. At low concentrations, the vertical offsets between the various curves of Fig. 4 were smaller than obtained from our argument by about a factor of 2, and were much less for the $p = 0.21$ and 0.23 curves. This discrepancy may occur when large clusters are present because the vacancy spends a large fraction of its time in the interior of the cluster. This reduces the number of opportunities for the vacancy to exchange with a bounding A atom and escape the cluster.

The strength probability, P, is not so important in interpreting our results. (Recall that P is the probability for an arbitrary site to belong to an infinite percolating cluster, and is nonzero only above p_c.) Although the vacancy may be placed initially on a nonpercolating cluster, the vacancy is able to find its way onto another cluster without too much

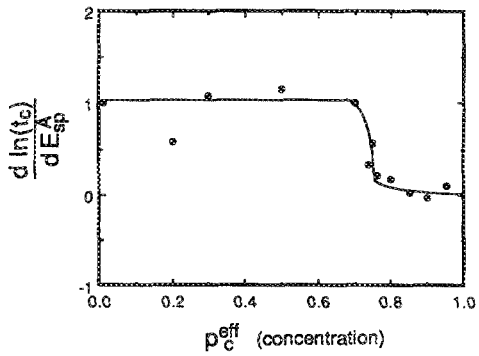

FIG. 6. Graphs of t_c vs E^A_{sp} were obtained for $l_c = 80$ for the case when $P^A_i = 1 \times 10^4 \exp(-E_{sp})$; $P^B_i = 1$. The graphs were straight lines for $E^A_{sp} \leqslant 5$. The data presented here are the slopes of these straight lines vs p^{eff}_c (B concentration). Line is drawn to guide the eye.

delay because the A atoms are allowed to move. A consequence of this is our observation that for different starting positions of vacancy, there was no significant change in the distance versus time data for vacancy migration. This unimportance of P is perhaps the greatest qualitative difference between our present work and the standard percolation theory. In the percolation theory, the only way for a vacancy to percolate is for it to be situated initially on an infinite percolating cluster; this is not a necessary condition for thermally activated diffusion.

Until now we have considered the A atom to be the slow species because it had the largest activation barrier for a diffusive jump. The pre-exponential factor can also be used to control the jump frequency, however, and an interesting case occurs when a large pre-exponential factor for the A atom makes it the fast species in spite of its larger activation barrier. Results from simulations of such cases at intermediate temperatures are presented in Fig. 6. From these data we see that the thermally activated jump of a fast A atom controls the rate of vacancy diffusion over a wide range of concentrations, but this is not so at concentrations below the percolation threshold of A atoms. The concentration dependence of the activation energy shown in Fig. 6 is quite the opposite to that of Fig. 5, where the temperature dependence occurs for compositions below the percolation threshold of the fast species.

The discontinuities in

$$d\,[\ln(t_c)]/dE^A_{sp}$$

in Figs. 5 and 6 indicate how p_c may influence diffusion experiments. Instead of looking for the presence or absence of diffusion, it may be possible to arrange a study of percolation phenomena by measuring the temperature dependence of diffusion coefficients above and below the percolation threshold. For such work we offer the caveat that the concentration dependencies of the pre-exponential factors of the solute diffusivities must not overcome the concentration dependencies of their Boltzmann factors, especially if this changes the identity of the more mobile species. Chemical interdiffusion in Nb-U may meet this qualification. A marked change in the activation energy for chemical interdiffusion was reported when the concentration of the faster U atoms exceeds 20 at. %,[16] and U is the more mobile species over a wide composition range. In most alloy systems there will also be nonzero interatomic interactions. Here order–disorder and clustering phenomena[17,18] must be considered, and it may prove necessary to consider p^{eff}_c as a function of local atomic order. For example, a weak clustering tendency could explain why the discontinuity in activation energy for chemical interdiffusion in Nb-U occurs below the *bcc* percolation threshold.

V. CONCLUSION

In Monte Carlo simulations of vacancy diffusion in *bcc* alloys, we explored the relationship between activation barrier heights for the vacancy-atom exchange and an effective percolation threshold concentration. The concentration threshold of percolation theory, p_c, is still a useful concept, and p_c remains unchanged in value when the slower atoms have a finite mobility. Percolation does occur below p_c, but it is impeded by the time required for the vacancy to move between clusters of mobile atoms. Because the vacancy is able to move between clusters of fast atoms even at low concentrations, the strength of the percolating cluster is a less important concept than in formal percolation theory. When the pre-exponential factors for the diffusivities of the two species are not concentration dependent, the difference in activation energy of the vacancy above and below the percolation threshold will equal the difference in activation energies of the two species. This may prove useful for identifying percolation phenomena in diffusion experiments.

ACKNOWLEDGMENTS

Assistance with the computer simulations by L. Anthony is acknowledged. This work was supported by the U. S. Department of Energy under Contract No. DE-FG03-86ER45270.

[1]S. R. Frisch and J. M. Hammersley, J. Soc. Indust. Appl. Math. **11**, 894 (1963).
[2]V. K. S. Shante and S. Kirkpatrick, Adv. Phys. **20**, 325 (1971).
[3]D. Stauffer, *Introduction to Percolation Theory* (Taylor and Francis, Philadelphia, PA, 1985).
[4]W. Y. Hsu, W. G. Holtje, and J. R. Barkley, J. Mater. Sci. Lett. **7**, 459 (1988).
[5]A. G. Khachaturyan, *Theory of Structural Transformations in Solids* (Wiley-Interscience, New York, 1983), p. 136.
[6]G. E. Murch and S. J. Rothman, Philos. Mag. A **43**, 229 (1981).
[7]J. R. Manning, *Diffusion Kinetics for Atoms in Crystals* (Van Nostrand, Princeton, NJ, 1968).
[8]J. R. Manning, Phys. Rev. B **4**, 1111 (1971).
[9]H. J. de Bruin, G. E. Murch, H. Bakker, and L. P. van der Mey, Thin Solid Films **25**, 47 (1975).
[10]R. Kikuchi and H. Sato, Phys. Rev. B **28**, 648 (1983).
[11]H. Bakker, in *Diffusion in Crystalline Solids*, edited by G. E. Murch and A. S. Norwick (Academic, New York, 1984).
[12]P. G. Shewmon, *Diffusion in Solids* (McGraw-Hill, New York, 1963).
[13]F. Lancon, L. Billard, W. Chambron, and J. Chamberod, J. Phys. **15**, 1485 (1985).
[14]T. Limoge and J. L. Bocquet, Acta. Metall. **36**, 1717 (1988).
[15]N. W. Ashcroft and N. D. Mermin, *Solid State Physics* (Holt, Rinehart & Winston, New York, 1976), p. 247.
[16]N. L. Peterson and R. E. Ogilvie, Trans. Metall. Soc. AIME **227**, 1083 (1963).
[17]N. A. Stolwijk, H. Bakker, and M. van Gend, J. Phys. C **13**, 5207 (1979).
[18]B. Fultz, J. Chem. Phys. **87**, 1604 (1987).